

Air coupled ultrasonic detection of surface defects in food cans

Fernando Seco, Antonio Ramón Jiménez and María Dolores del Castillo
Instituto de Automática Industrial, CSIC.
Ctra. de Campo Real, km 0.200, 28500 Arganda del Rey, Madrid, Spain

Corresponding mail: fseco@iai.csic.es

This paper appears in *Measurement Science & Technology*, vol. 17, pp. 1409-1416 (2006).

Copyright: Institute of Physics and IOP Publishing Limited 2006

Abstract

In this paper we describe an ultrasonic inspection system used for detection of surface defects in food cans. The system operates in pulse-echo mode and analyzes the 220 kHz ultrasonic signal backscattered by the object. The classification of samples into valid or defective is achieved with χ^2 statistics and the k -nearest neighbour method, applied to features computed from the envelope of the ultrasonic echo. The performance of the system is demonstrated empirically in the detection of the presence of the pull tab on the removable lid of easy-open food cans, in a production line. It is found that three factors limit the performance of the classification: the misalignment of the samples, their separation of the ultrasonic transducer, and the vibration of the conveyor belt. When these factors are controlled, classification success rates between 94 and 99 % are achieved.

Keywords: Ultrasonic inspection, quality control, signal processing.

1 Introduction

Ultrasonic sensors are commonly used for monitoring industrial processes [1], for example as counters of items on a conveyor belt, presence detectors, liquid level measurement, flowmeters, etc. Besides these relatively simple tasks, advances in sensor technology and signal processing permit to use ultrasonic technology for more complex purposes, like the study of the surface of objects, and thus be useful for sample classification or detection of surface defects. In this aspect, ultrasound-based inspection techniques can be competitive with standard techniques like computer vision, with the advantages of low cost, short inspection times, small computational requirements, and minimum interference with existing industrial setups. Besides, they can be operative for the inspection of objects with

low visual contrast, or in low light or dusty environments where computer vision systems might experience difficulties.

Much research is reported in the literature regarding ultrasonic surface inspection techniques. Martín [2] used 220 kHz piezoelectric transducers to distinguish between the flip sides of a coin by decomposition of the ultrasonic signal and correlation with previously stored reference templates. Error rates of about 1 % are obtained in laboratory conditions, which include positioning of the object in an optical bedplate, reduction of vibration and air motion, and signal averaging. Fritsch [3] also achieved a high success rate in the classification of six simple objects in static operation, using a single emitter-receiver 220 kHz transducer. In this system the ultrasonic signal is first deconvolved to find the impulse response and increase the spatial resolution, and the peak and width of the ultrasonic signals are used for the classifying process. This technique is well suited for the kind of samples chosen for the demonstration, which are stepped objects of different heights. Caicedo [4] built an object classifier system which worked by extracting a set of features (parameters) of the envelope of the reflected ultrasonic echoes. Two classification experiments are described in his work: the first is a set of cylinders with diameters ranging from 52 to 60 mm, and the second a set of gears with 24 to 44 teeth. In both cases close to 100 % of success is achieved; however, a static configuration is used, with the pieces being carefully positioned in an optical bench.

The use of multi-transducer arrays permits to extract more information about the object under study. For example, Lázaro [5] employed an array of nine 40 kHz emitters and receivers for detection of notches and grains of 5 mm in brake drums and discs. By extracting a set of parameters (like amplitude peak, time of arrival of the pulse, etc) from the envelope of the ultrasonic echoes, and processing the data with a neural network, a defect detection capability above 80 % was obtained. Long processing times (about 10 s) and the need for a careful positioning of the piece under study are pointed out in their work. Watanabe [6] has used an 8×8 transducer receiver array operating at 40 kHz and a single emitter. For each received signal, the amplitude and phase are computed, and the resulting matrix processed via the inverse Fourier transform to reconstruct an acoustical image of the object. The data is fed into a neural network which permits classification of a set of 26 different objects (shaped as the alphabet letters). The success rate ranges between 90 and 100 % but drops to 75 % when the letters are rotated in random angles.

Finally, ultrasonic scanning (either mechanical or electronic) and focusing of the ultrasonic signals can be used to produce images of the objects of high quality, ultimately limited by diffraction. Lach [7] uses a broadband (80-280 kHz) transducer to scan the piece under study along a line, obtaining a set of 220 points for each object (in the two-dimensional frequency-angle space); and principal component analysis and the k -nearest neighbour techniques for feature selection and classification. Three objects of thickness 0.5 mm are classified with a success rate of 85-96 %, allowing for 10 mm displacements and up to $\pm 6^\circ$ rotations. Brudka [8] uses an array of 40 ultrasonic emitter/receiver pairs working at 150 kHz to form images of objects in a conveyor belt, which are processed by a neural network to assist a robotic arm in the task of grasping the object. In the system described by Robertson [9] wideband capacitive transducers with a cylindrical geometry operating at 500 kHz were used to produce a high quality image of a coin, with axial resolution on the order of 5 μm and lateral resolution under 1 mm. Acquisition and processing of the ultrasonic signals are reported to last several hours.



Figure 1: Food cans with and without the “easy-open” pull tab on the top cover.

Most of the authors cited above have noted the high sensibility of the ultrasonic systems to vibrations and the need for careful positioning of the examined objects; factors which are disadvantageous for their use in practical industrial problems. In this paper we introduce an ultrasonic inspection system based on a single emitter/receiver transducer, demonstrate its performance in a quality control problem from the food industry, and study the limitations set up on its performance by the perturbing factors indicated above.

2 Problem definition

The ultrasonic inspection technique will be applied to an industrial quality control process: checking the presence of the pull tab in easy-opening food packages (see figure 1). During the manufacture of the can, the pull tab is attached to a rivet which has been formed on its top cover; any failure in that process may cause metal fracture of the rivet or the scoreline (the thinner line along the perimeter of the can cover). The presence and correct positioning of this pull tab should be checked previous to the packaging of the can, because otherwise the product might be difficult to open or its contents might leak out.

Typically this problem is solved with computer vision; however we will show in this paper how it can be handled efficiently with ultrasonic technology. For this purpose we installed an inspection station in a section of production line, which consists of a 90 mm wide cardanic belt. The diameter of the can is 65 mm, and they are transported at a speed of approximately 0.5 m/s. The measured height of the pull tab ring over the top surface of the can is 2.4 mm.

3 System description

3.1 Inspection station

The ultrasonic inspection station (see figure 2) is placed on a chassis mounted on top of the transporting belt. The ultrasonic transmitter/receiver is a piezoelectric transducer by Massa Products Co., model E-188/220, operating at 220 kHz and with a bandwidth of 25 kHz. Errors caused by lateral displacements of the items are minimized by a careful

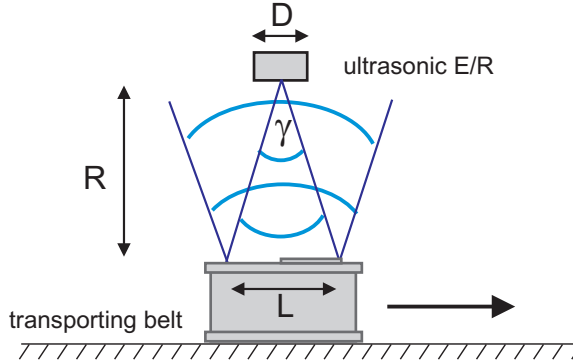


Figure 3: Pulse-echo procedure for object identification.

3.2 Physical constraints

Several physical constraints must be considered in the design of a pulse-echo ultrasonic inspection system [10]. The resolution attainable in the axial and lateral directions depends on the ultrasonic frequency f_0 — higher frequencies permit smaller defects to be detectable [9]. However, the attenuation α of the ultrasonic wave increases as the frequency squared, which quickly degrades the signal to noise ratio (SNR) and the repeatability of the measurements; for that reason, air coupled ultrasonic systems usually operate at frequencies below 1 MHz. Considering the setup of figure 3, the sound pressure level (SPL) of the reflected wave decreases steeply with the separation R :

$$\text{SPL}(R) = \text{SPL}_0 - 20 \log_{10}(2R/R_0) - (20 \log_{10} e)\alpha(2R - R_0) \quad \text{dB}, \quad (1)$$

where SPL_0 and R_0 are reference levels, as given in the manufacturer's datasheet. At 220 kHz, the attenuation coefficient is $\alpha = 8.7$ dB/m.

The axial resolution, as well as the effective SNR, can be enhanced by the processing gain obtained by modulating and coding of the ultrasonic signal. This might be needed in situations of great attenuation of the ultrasonic signal; for example, chirp signals are used in the examination of the contents of food cans to compensate for the great attenuation caused by through transmission of ultrasonic pulses [11]. In our application, with relatively high SNR, we have used a simple 5 cycle pulse train.

The area insonified by the ultrasonic pulse (with diameter L in figure 3) is related to the transducer diameter D and the distance to the object R by:

$$L = 2R \tan \gamma/2, \quad (2)$$

where the angle γ is, in the flat piston approximation [12]:

$$\sin \gamma/2 = 0.514c/Df, \quad (3)$$

with c being the speed of sound. From these equations, an increase in frequency corresponds to a smaller covered area. Summarizing, there exists a tradeoff between three

relevant parameters of the ultrasonic inspection technique: scanned area (size of the inspected object), axial resolution (size of the detectable defect) and SNR (repeatability between samples).

In our case, the emission/reception lobe is measured to be $\gamma = 10^\circ$ (-3 dB), which, for a transducer-object separation of $R = 100$ mm, corresponds to an insonified region of diameter $L = 17$ mm. The length of the pull tab is 35 mm, and it is attached to a point close to the perimeter of the can, so in conditions of good centering of the ultrasonic transducer, this setup guarantees that a significant portion of the pull tab will be insonified and provides a good balance between covered area and SNR.

3.3 Signal Processing and Parameter Extraction

After signal acquisition, the ultrasonic echo is processed to extract the parameters which will serve for the classification process. The first step consists in eliminating the ultrasonic carrier of frequency f_0 , using the Hilbert transform to compute the complex envelope of the acquired signal. This process is carried out in the computer, but future industrial prototypes can benefit from standard in-phase/quadrature demodulators, or efficient DSP-based implementations [13], for this task.

Several choices for the definition of the parameter set are reported in the literature. Legendre [14], working in ultrasonic Non Destructive Testing of plates, performs a wavelet decomposition of the envelope of the ultrasonic wave and uses as parameters the amplitude coefficients; other authors [15] prefer an orthogonal basis formed by a set of Laguerre functions, which are well suited for the typical ultrasonic waveforms found in air applications. We have found that the following set of parameters, which have physical meanings, yields good classification results:

- Maximum (Max) value of the envelope, in V.
- Time of flight (TOF) of the ultrasonic echo, obtained by linear fitting of a set of discrete points of the rising edge of the envelope of the ultrasonic echo. It is measured in μs .
- Mean slope (S) of the rising edge of the signal, obtained also by linear fitting. It is normalized by the parameter Max, and measured in $(\mu s)^{-1}$.
- Energy (E) of the wave, computed by summing the squares of all the discrete points of the envelope, and measured in V^2 .

As was mentioned in section 3.1, for each can, two different pulse-echo emissions are performed (corresponding to slightly displaced snapshots of the same object), and therefore the feature vector x for every item is constructed as:

$$x = [\text{Max}_1 \quad \text{TOF}_1 \quad S_1 \quad E_1 \quad \text{Max}_2 \quad \text{TOF}_2 \quad S_2 \quad E_2]^T. \quad (4)$$

The classification methods described in the next section are based in the distance between samples, and for that reason the parameters of equation 4 are scaled by their respective variances so that they become adimensional and with relative equal magnitude.

3.4 Classification

The classification problem consists in mapping points of the feature space defined by the parameters into a limited number of classes [16]. For the problem considered in section 2 the classifier is reduced to a decision between only two classes: with and without pull tab. Following the practice of the decision theory, we designate by H_0 the hypothesis that the can has the pull tab, and by H_1 the hypothesis that the pull tab is missing. The performance of the classification system is measured by two statistical parameters: the detection probability P_d (the correct detection of the event H_1); and the false alarm probability P_{fa} (the case that the tab was correctly positioned, but the system chose hypothesis H_1 instead of H_0). A general decision strategy based on the Neyman-Pearson criterion [17] depends on whether the *a priori* probabilities $P(H_0)$ and $P(H_1)$ are known (or can be estimated from the data), as well as on the costs associated with the classification errors for the classes H_0 and H_1 .

Two decision algorithms are considered in this paper. The first is based on a χ^2 statistics centered on one of the hypotheses. By considering the class with smaller variance of the data, which empirically is found to be the set H_1 of samples without the pull tab, we can compute the covariance matrix:

$$C_1 = \mathcal{E}\{(x_1 - \bar{x}_1)(x_1 - \bar{x}_1)^T\},$$

where $\mathcal{E}\{\cdot\}$ is the expectation operator and $\bar{x}_1 = \mathcal{E}\{x_1\}$ is the vector parameter mean of the samples of class H_1 . Then the Mahalanobis distance r^2 of a new sample with parameter vector x to the center of the class H_1 is [16]:

$$r^2 = (x - \bar{x}_1)^T \text{inv}[C_1](x - \bar{x}_1). \quad (5)$$

The distance r^2 follows a χ^2 distribution function, with a number of degrees of freedom equal to the number of parameters of vector x defined in equation 4, and can be used to discriminate between classes H_0 and H_1 . The threshold r_{th}^2 which separates the probability density functions $P(r^2|H_0)$ and $P(r^2|H_1)$ is taken according to the Neyman-Pearson criterion mentioned above.

The second technique used in this paper is a machine learning algorithm: the k -nearest neighbour classification method [16]. In this method we store a number K of known parameter samples for each class. When a new can is evaluated, the distances of the sample vector to the $2K$ stored reference vectors are computed, and the k samples with minimum distance are extracted. The sample under evaluation is assigned to the class which has more elements in this k -neighbours reduced set.

The performance of both methods for our classification problem is studied experimentally in the next section.

4 Empirical Results

A typical ultrasonic signal reflected from a can with the experimental setup described in the last section is shown in figure 4. The dead zone corresponds to the coupling of the emission and reception processes. We show the portion of the waveform used in the

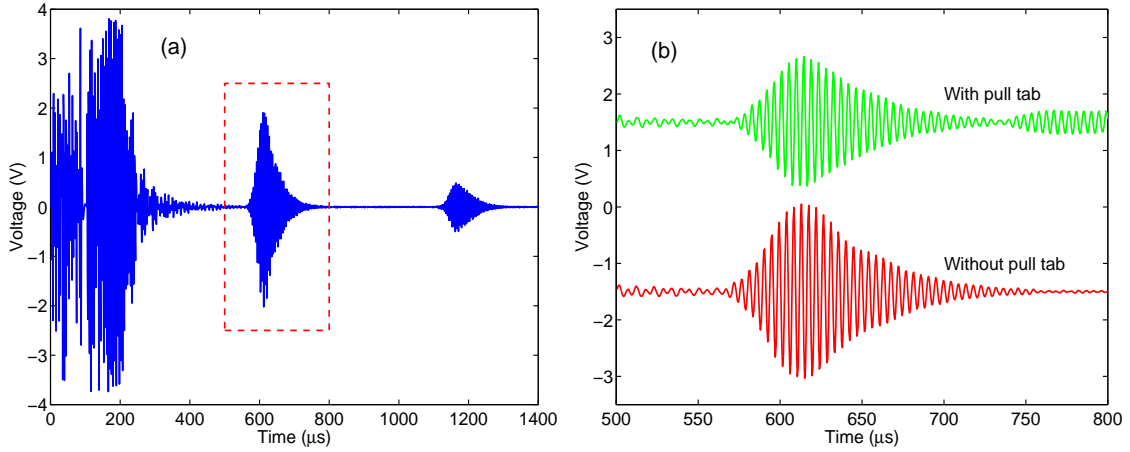


Figure 4: Typical echo signal received from a can. Part (a) shows the complete echo waveform, with the dead zone, the signal used for the analysis (dashed box) and a secondary echo caused by a reflection on the support of the transducer. In part (b) we show echoes from cans with and without the pull tab on the top cover.

computation of the parameters and typical signals for cans with and without the pull tab.

A set of 12 different cans, half of them with the pull tab correctly positioned on the opening lid and the rest without it were placed on the transporting belt, which was kept functioning until 1200 measurements were completed. Scatter plots of the set of parameters defined in section 3.3 are shown in figure 5 (only the parameters corresponding to the first ultrasonic emission are shown). The variance of the parameters corresponding to cans with the pull tab (H_0) is higher than of those without it. This can be attributed to variations of the height of the pull tab from one can to the next, to the small lateral displacements permitted by the alignment device, and by the fact that the inspection system does not control the angular orientation of the can.

We used the Principal Component Analysis (PCA) method [16] to determine which combination of parameters yielded maximum separability. It was found that the most discriminative parameters were the slope S and the time of flight TOF , while inclusion of the energy E yielded marginal improvement, and that of the maximum Max none at all. As a result, in the remaining of this paper, the following parameter vector will be employed: $x = [S_1 \quad TOF_1 \quad S_2 \quad TOF_2]^T$.

4.1 Comparison of classification methods

The χ^2 statistics is used first in the classification process; as it was discussed above, it is preferable to use the most compact class in the feature space (H_1), as a center for the discrimination. 120 samples were used to compute the statistical parameters (mean vector and covariance matrix) of class H_1 . the results of the χ^2 classification process are shown in the first entry of table 1 and graphically in figure 6. The threshold for separation between classes H_0 and H_1 is chosen at the point where $P(r^2|H_0) = P(r^2|H_1)$, which maximizes the probability of correct classification assuming that cans with and without pull tab are

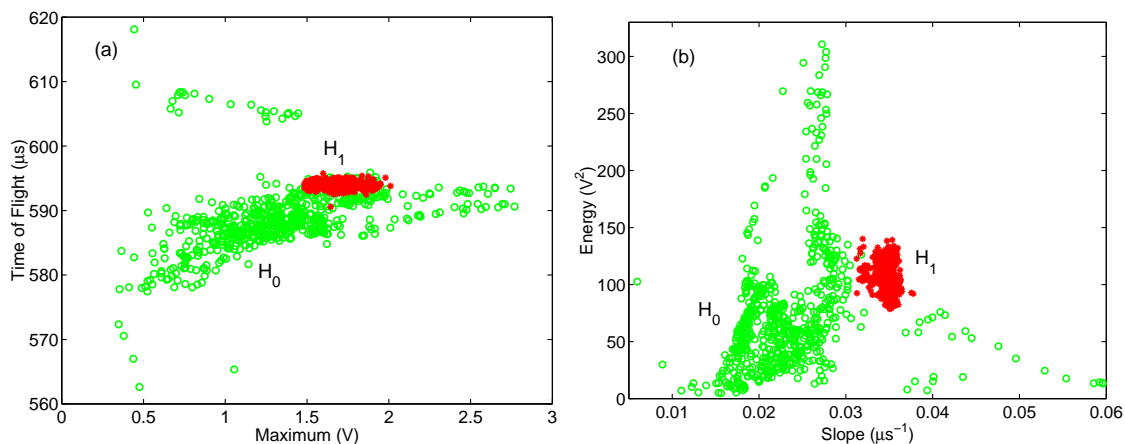


Figure 5: Scatter plots of the parameters: (a) maximum (Max) versus time-of-flight (TOF); and (b) slope (S) versus energy (E). Cans with pull tab (o) and without pull tab (*).

equally likely to be present. Under these conditions, the detection probability is found to be $P_d = 0.995$, and the false alarm probability $P_{fa} = 0.001$, with a total classification success of 0.994. The probability density functions of the classes H_0 and H_1 in figure 6 are clearly separated.

For comparison, the same data is analyzed with the k -nearest neighbours method. The number of reference samples is $2K = 120$ samples, half from each class; from this set, the $k = 5$ nearest neighbours are considered in the decision. The results are a detection probability $P_d = 0.998$ and a false alarm probability $P_{fa} = 0.058$, with a correct classification rate of 0.940. In figure 7 we show the scatter plot of the parameters, with the missclassified samples marked in black, and a histogram of the number of neighbours for each class. As can be seen, some of the cans with pull tab are actually closer (in the feature space) to those without the pull tab, causing a relatively high percentage of false alarm errors. Due to its better performance, we will use only the χ^2 statistical method for the remaining of this paper.

4.2 Sensibility to transporting conveyor speed and separation

As was stated in section 3.2, the classification of objects with ultrasonic sensors is very sensitive to the transducer-object distance, as well as to vibrations of the transporting element; these effects are analyzed in this section.

Increasing the separation between the transducer and the object under study decreases the SNR and, as a consequence, the repeatability between samples. In figure 8 and the second row of table 1 we show the effect of rising the transducer by 47 mm, which, according to equation 1, causes a signal drop of 10 dB. The performance of the classification algorithm falls to $P_d = 0.940$ and $P_{fa} = 0.085$ (total classification success of 0.855) as the scatter plots of the parameters overlap partially.

Changes in the transporting speed have a more drastic effect on the ultrasonic signals, because they cause vibrations of the sample, and further spread the parameters scatter

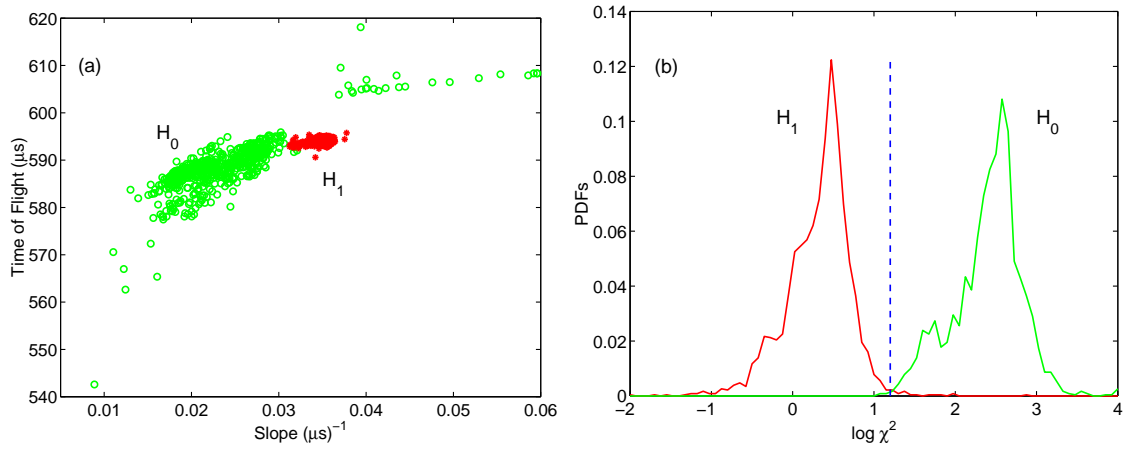


Figure 6: Scatter plots of the parameters slope (S) and time-of-flight (TOF), and PDFs $P(r^2|H_0)$ and $P(r^2|H_1)$ for a low separation, low speed situation. Cans with pull tab (\circ , ---) and without pull tab ($*$, ---).

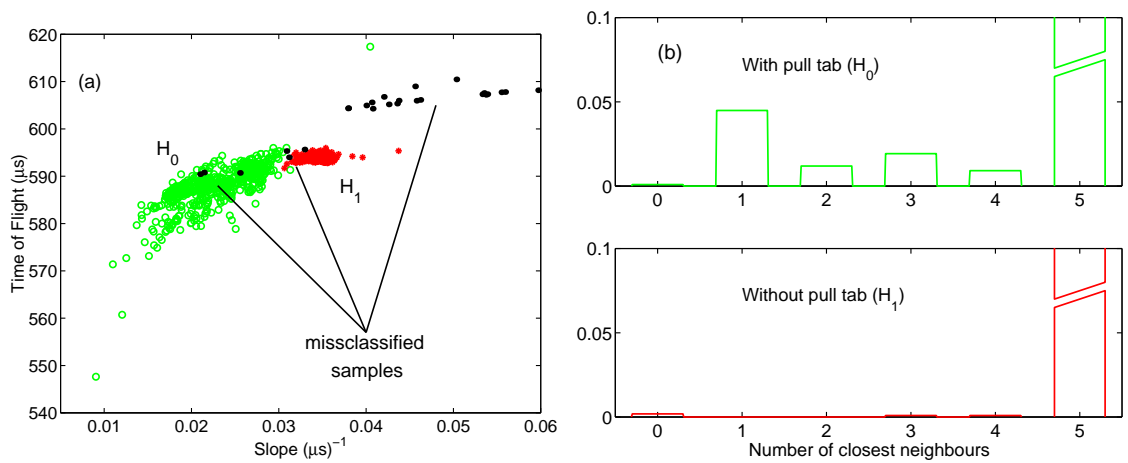


Figure 7: Results of the k -nearest neighbours algorithm. In the scatter plot (a) the misclassified samples are marked with black dots. The histogram (b) shows the statistical distribution of nearest neighbours for the samples of classes H_0 and H_1 . A part of the H_0 (green) samples are actually closer to samples of class H_1 , causing a relatively high false alarm probability P_{fa} .

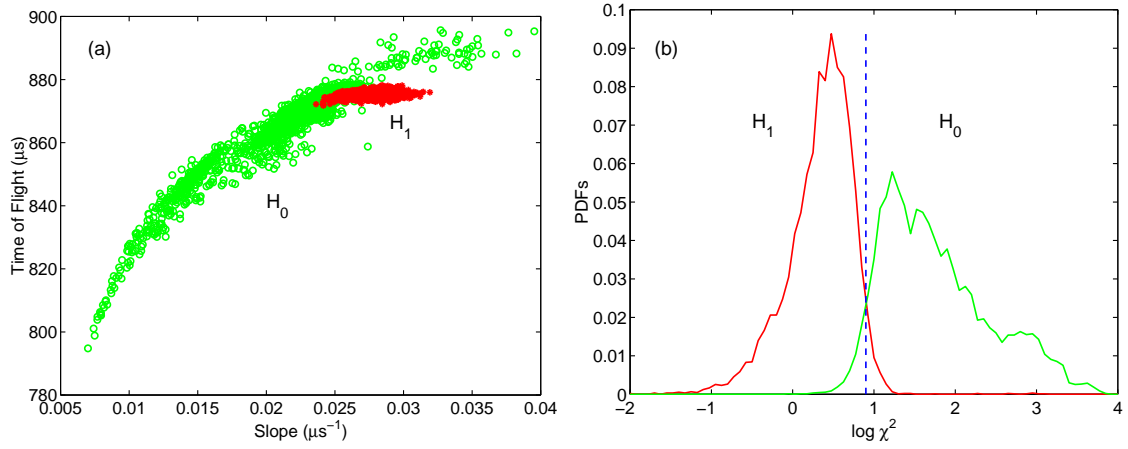


Figure 8: Scatter plots of the parameters slope (S) and time-of-flight (TOF), and PDFs $P(r^2|H_0)$ and $P(r^2|H_1)$ for a high separation situation. Cans with pull tab (o, —) and without pull tab (*, —).

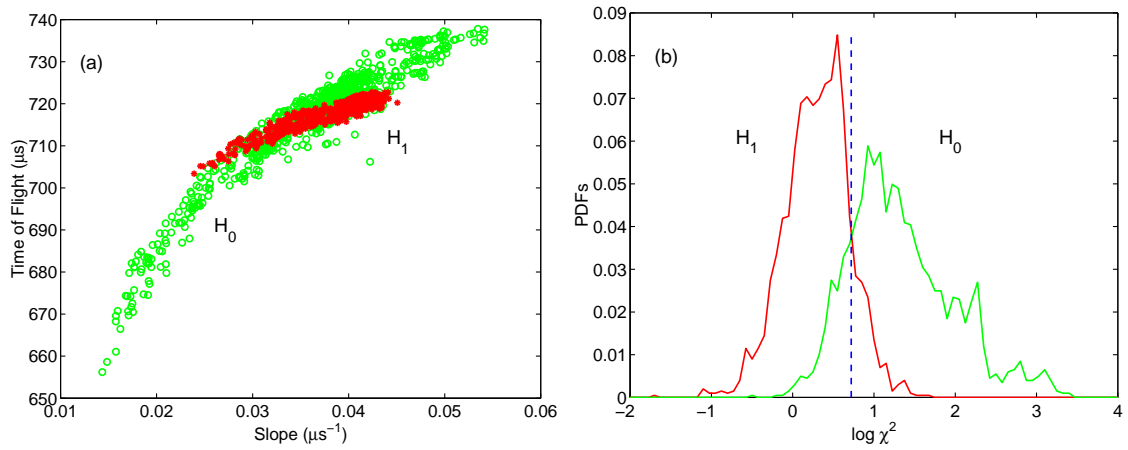


Figure 9: Scatter plots of the parameters slope (S) and time-of-flight (TOF), and PDFs $P(r^2|H_0)$ and $P(r^2|H_1)$ for a high velocity situation. Cans with pull tab (o, —) and without pull tab (*, —).

Table 1: Results of the χ^2 classification process in three different cases. The columns correspond to: speed of the conveyor belt, separation between transducer and can, standard deviations of the parameters slope and time of flight (for cans with and without pull tab), and the obtained probabilities of detection, false alarm, and correct sample classification.

Speed (m/s)	Separation (mm)	σ_S (μs^{-1})		σ_{TOF} (μs)		P_d	P_{fa}	$P_d - P_{\text{fa}}$
		with	without	with	without			
0.40	101	0.0068	0.0011	6.1	0.58	0.995	0.001	0.994
0.44	148	0.0043	0.0012	13	1.1	0.940	0.085	0.855
0.54	122	0.0070	0.0038	12	3.2	0.873	0.154	0.719

plots. When the speed of the conveyor belt is increased by 35 % (from 0.40 m/s to 0.54 m/s), we obtain the results shown in figure 9. The probability of correct detection drops to only $P_d = 0.873$ with a false alarm probability of $P_{\text{fa}} = 0.154$ and a total classification success of 0.719.

The results of the three experiments are summarized in table 1. For the cans with the pull tab the parameters have always high variance, but do not change significantly with the speed of the belt, so our interpretation is that they are due to the changes of position and orientation of the samples with respect to the ultrasonic transducer. The corresponding values for cans without the pull tab are 2–10 times lower, but they increase sharply with the conveyor belt speed, which seems to indicate that they are caused by the vibrations of the samples.

In any case, it is clear that the performance of the ultrasonic inspection system degrades with the transporting speed and the transducer/object distance. The first factor is certainly an obstacle for industrial applications; however a conveyor belt with less vibration and controlled positioning can be designed for placement of the items at the point of ultrasonic inspection (in this sense, the cardanic belt used in the research described in this paper is not the most favorable transporting mechanism). The second factor sets up a limit on the size of the object which can be covered with a single transducer emission. Possible solutions to cover larger objects include scanning of the area with several consecutive emissions or the use of more transducers—this approach is feasible due to the relative low cost of ultrasonic sensors and their related electronics.

5 Conclusions

In this paper we have described and built an ultrasonic inspection system and used it for surface examination of food packages in a production line. Under controlled conditions of speed and alignment of the samples, the system shows up to 99 % success in the problem of determining the presence of the pull tab ring in food cans.

The experimental work with the inspection station confirms that three factors control the performance of the ultrasonic system: alignment of the samples under study with respect to the transducer, separation between sample and transducer, and, most importantly, the vibrations set up by the conveyor belt. A proper design of the industrial transporting mechanism can overcome these difficulties, and, under this assumption, ultrasonic surface inspection can be cost and performance-wise competitive with other technologies like

computer vision.

Acknowledgement

F. Seco wants to acknowledge the support by the Torres Quevedo research program from Spain's Science and Technology Ministry during the completion of this work.

References

- [1] Peter Hauptmann, Niels Hoppe, and Alf Puttmer. Application of ultrasonic sensors in the process industry. *Meas. Sci. Technol.*, 13:R73–R83, 2002.
- [2] J. M. Martín Abreu, T. Freire Bastos, and L. Calderón. Ultrasonic echoes from complex surfaces: an application to object recognition. *Sensors and Actuators A*, 31:182–187, 1992.
- [3] C. Fritsch, J.J. Anaya, A. Ruiz, and L.G. Ullate. A high-resolution object recognition ultrasonic system. *Sensors and Actuators A*, 37-38, 1993.
- [4] E. Caicedo, L. Calderón, and R. Ceres. A new approach to object classification using ultrasonic sensors. In *Workshop on Industrial Automation, ECLA '94*, 1994.
- [5] A. Lázaro and I. Serrano. Ultrasonic recognition technique for quality control in foundry pieces. *Meas. Sci. Technol.*, 10(9):N113–N118, 1999.
- [6] Sumio Watanabe and Masahide Yoneyama. Ultrasonic robot eyes using neural networks. *IEEE Trans. on Ultrasonics, Ferroelectrics and Frequency Control*, 37(2):141–147, May 1990.
- [7] M. Lach and H. Ermet. An acoustic sensor system for object recognition. *Sensors and Actuators A*, 25-27, 1991.
- [8] Marek Brudka and Andrzej Pacut. Intelligent robot control using ultrasonic measurements. *IEEE Trans. on Instrumentation and Measurement*, 51(3):454–459, June 2002.
- [9] T. J. Robertson, D. A. Hutchins, and D. R. Billson. Capacitive air-coupled cylindrical transducers for ultrasonic imaging applications. *Meas. Sci. Technol.*, 13(5):758–769, 2002.
- [10] W. Manthey, N. Kroemer, and V. Magori. Ultrasonic transducers and transducer arrays for applications in air. *Meas. Sci. and Technol.*, 3(3):249–261, 1992.
- [11] T. H. Gan, D. A. Hutchins, and D. R. Billson. Preliminary studies of a novel air-coupled ultrasonic inspection system for food containers. *Journal of Food Engineering*, 53(4):315–323, 2002.
- [12] David T. Blackstock. *Fundamentals of Physical Acoustics*. Wiley Interscience, 2000.
- [13] Angelo M. Sabatini and Alessandro Rocchi. Sampled baseband correlators for in-air ultrasonic rangefinders. *IEEE Trans. on Industrial Electronics*, 45(2):341–350, April 1998.

- [14] S. Legendre, D. Massicotte, J. Goyette, and T. K. Bose. Neural classification of Lamb wave ultrasonic weld testing signals using wavelet coefficients. *IEEE Trans. on Instrumentation and Measurement*, 50(3):672–678, June 2001.
- [15] Angelo M. Sabatini. A digital signal-processing technique for ultrasonic signal modeling and classification. *IEEE Trans. on Instrumentation and Measurement*, 50(1):15–21, February 2001.
- [16] Peter E. Hart Richard O. Duda and David G. Stork. *Pattern Classification*. Wiley-Interscience, 2 edition, 2000.
- [17] John Minkoff. *Signals, Noise and Active Sensors*. Wiley Interscience, 1 edition, 1992.